A Passive Displacer for a Stirling Pulse Tube Cryocooler

H. Rana, M.A. Abolghasemi, R. Stone, M. Dadd, P. Bailey

Department of Engineering Science, University of Oxford
Oxford, OX1 3PJ United Kingdom

ABSTRACT

Stirling pulse tube cryocoolers (SPTCs) can operate by incorporating a displacer into the warm end of a pulse tube cryocooler. Previous studies have shown that SPTCs running with an active displacer demonstrate good performance and higher efficiencies than pulse tube cryocoolers that utilize inertance tubes. Having an actively driven displacer requires a second phase from the power electronics, and the extra motor and electrical feedthrough adds to the complexity of the design, so it is desirable to have a passively driven displacer. This study presents the analysis and design of a passive displacer driven by the pressure difference across the displacer piston. A harmonic analysis and design of the displacer unit was completed, in conjunction with a numerical model constructed in Sage. This permitted the correct characteristics for the displacer to be designed in order to operate with the existing compressor and cold head. This included testing and analysis of different spring assemblies, optimisation of the displacer dimensions, and the piston moving mass. The passive displacer will replace the active displacer in an existing 80 K coaxial SPTC.

INTRODUCTION

Stirling pulse tube cryocoolers (SPTCs) allow detectors and other electronic devices to reach cryogenic temperatures for a number of scientific and industrial applications. The efficiency of the SPTC performance is governed by the intricate interplay between the mass flow and pressure pulse throughout the pulse tube, which can be controlled and fine-tuned by expanders and displacers at the warm end, as well as inertance tubes and orifices. SPTCs using active displacers permit the expansion (PV) power to be recovered from the warm end of the pulse tube back into the system, and as such, have been reported to reach higher efficiencies than those that make use of inertance tubes or orifices [1]. Using an active displacer introduces a second phase from the power electronics into the system and involves a more complicated design in order to incorporate the second motor or generator. It is therefore favorable to use a warm end displacer that is driven passively. To achieve the same operation and efficiency, a series of design analyses must be conducted to ensure the displacer dynamics match that of a comparable SPTC with an active displacer [2]. This paper presents a summary of the work completed to characterize the displacer dynamics and theoretically design its key components, using inputs from the coaxial SPTC with an active displacer performance. A design layout and harmonic analysis of the displacer is presented. Furthermore, a spring design consisting of Finite Element analysis and experimental testing to ascertain fatigue limits and the

Cryocoolers 21, edited by R.G. Ross, Jr., J.R. Raab and S.D. Miller

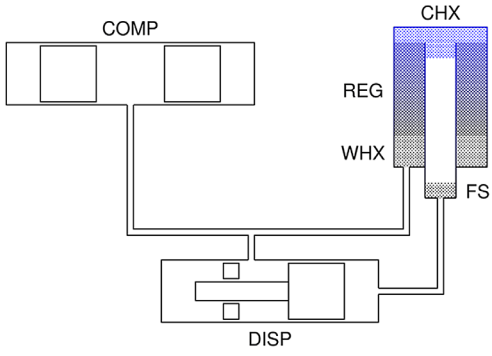

Figure 1. A coaxial cryocooler with an active displacer. COMP is the compression unit, DISP is the displacer, WHX is the warm end heat exchanger, PT is the pulse tube, CHX represents the cold head heat exchanger, REG is the regenerator, and FS is the flow straightener.

spring stiffness are presented. The outputs of these analyses provide design values for the displacer shaft diameter, spring stiffness, spring fatigue limit and stress regions, and displacer moving mass, enabling the manufacture and testing of a passive displacer for a high efficiency experimental coaxial SPTC.

STIRLING PULSE TUBE WITH DISPLACER

Active Displacer

The coaxial SPTC design is shown in Figure 1. The pulse tube is positioned inside the coaxial regenerator, and the displacer operation feeds into the system at the warm end of the pulse tube. The compressor and displacer units both have their own independent moving coil motors, and the motion of both is measured using linear variable differential transformer (LVDT) displacement transducers. This enables the amplitude of the oscillatory motion of both the compressor and displacer to be measured separately, as well as the phase angle of the displacer motion relative to the compressor. In the active design, the ability to fine tune both these motions permits reaching the optimal phase angle between the two. This enables a more efficient operation of the SPTC and is a particular benefit of an actively driven displacer.

Passive Displacer

Using an active displacer poses certain significant disadvantages - the power electronics introduce a second phase, and the incorporation of the second motor adds complexity to the design of the overall system. The latter introduces further vibrations at the cold end which are highly undesirable, considering the increasingly stringent vibration tolerances for the devices being cooled. It is therefore desirable to aim to reduce the mass and the number of additional moving parts, as well as simplify the cryocooler design. This improves reliability and longevity of the cryocooler. Inertance tubes can be utilized to achieve this, however, they do not recycle power back into the cryocooling system. A passively driven displacer is therefore a suitable solution to address each of these issues.

The passive displacer is driven by the pressure difference across the displacer piston and displacer shaft which is created by the compressor unit. The passive displacer requires designing such that it operates at the optimal conditions in conjunction with the compressor to reach a similar efficiency and operation as the active coaxial SPTC. Inputs from the coaxial SPTC using an active displacer, which has the same design dimensions and materials of all other key components, are therefore required to perform design analysis of the passive displacer. Figure 2 indicates the simulated output of the coaxial SPTC with an active displacer, showing how the displacer shaft power varies with phase angle of the displacer relative to the compressor. Positive shaft power indicates the displacer is receiving work and negative indicates that it is putting work into the system. Negative values for shaft power of the displacer are obtained at lower phase angles, and the point of intersection at the axis indicates the conditions for phase angle in which the displacer would be running passively.

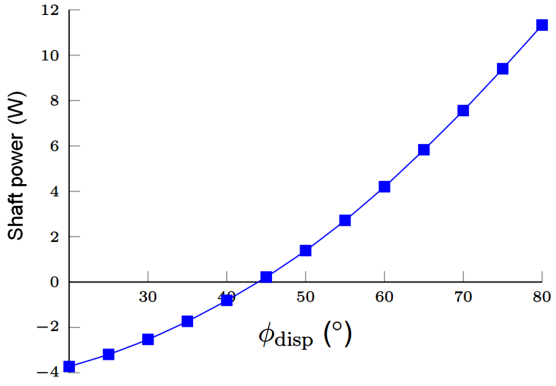

Figure 2. Simulated displacer shaft power with varying compressor-displacer phase angle ($Ø_{disp}$) for a comparable coaxial SPTC with an active displacer. The compressor stroke is 9 mm, operating frequency is 60 Hz, and fill pressure is 28 bar.

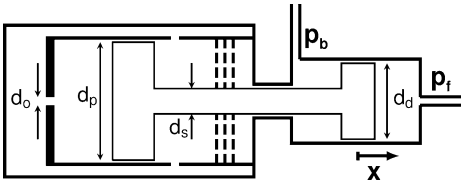

Figure 3. Schematic of the passive displacer.

DESIGN ANALYSIS

Displacer Design

A schematic of the passive displacer is shown in Figure 3. It shows a displacer piston of diameter d_d oscillating with displacement x due to the difference in pressure between the front space at p_f and the back space at p_b and the pressures either side of the damping piston. The displacer shaft with diameter d_s is connected to a damper piston of diameter d_p on the other side. The space in front of the damper piston is sealed from the rest of the back volume via an orifice plate of diameter d_o. Hence, the level of damping can be controlled by varying the size of the orifice. The dashed lines represent flexure bearings which are adjusted to achieve the necessary stiffness. Altogether, by varying the spring stiffness, moving mass, damping and shaft diameter we can ensure that the passive displacer operates at the optimal phase and stroke in order to maximise cooling and efficiency.

Harmonic Analysis

A phasor analysis for the displacer was completed in which all forces acting on the displacer were balanced. The forces that make up the total force, F_t, are shown in Equation 1, where F_m is the motor force, F_P is the gas spring force, F_s is the spring force, F_d is the damping force, α is the motor force constant, I is the current, ΔP is the pressure difference across the displacer piston, A is the surface area of the piston, k is the spring constant, and c is the damping coefficient. As the different forces act sinusoidally, they can be converted to phasor form, where the steady state solution for the displacement, x, is given by Equation 2, and ω is the angular frequency. Equation 3 indicates the full force balance in phasor form, where the $e^{i\omega t}$ components cancel.

$$F_t = F_m - F_P - F_s - F_d = mx = \alpha I - \Delta PA - kx - cx \quad (1)$$

$$x = x_1 e^{i\omega t} \quad (2)$$

$$\alpha I = kx + ic\omega x + \Delta PA - m\omega^2 x \quad (3)$$

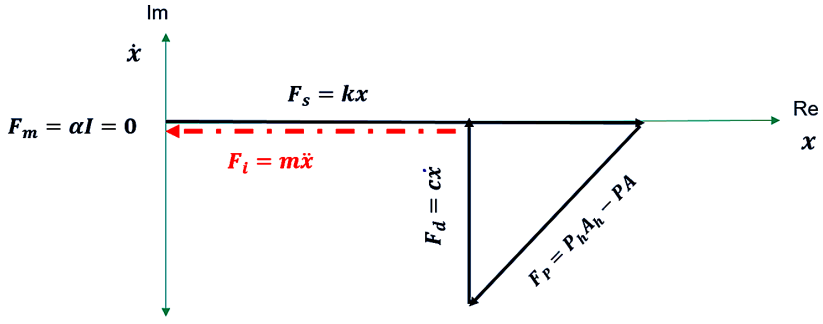

Figure 4. A typical phasor diagram for the forces acting on a displacer. When the forces balances to give a motor force F_m of zero the displacer is running passively.

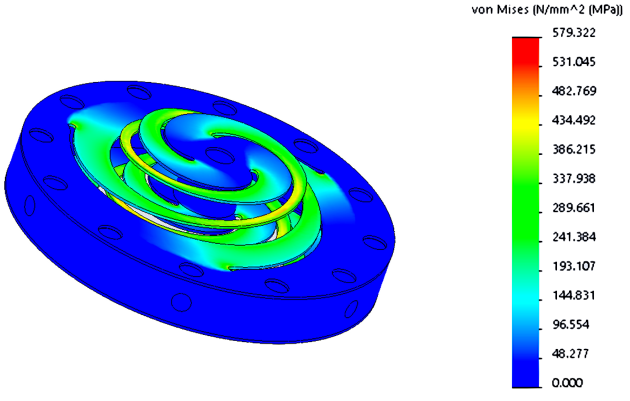

Figure 5. von Mises stress plot of the spring.

A phasor diagram, as shown in Figure 4, can be produced to diagrammatically represent the magnitude of all forces acting on the displacer in the real and imaginary axes [3]. This allows for the resultant force F_m to be determined. The necessary value for the shaft diameter of the displacer can be determined to achieve a motor force of zero. At F_m =0, the displacer is being run passively and does not require a motor.

FE Analysis of Springs

Finite Element (FE) analysis of the spring was undertaken to determine the regions of highest stress in the spring as well as the spring stiffness. The design stroke is known from the performance analysis completed for the coaxial SPTC with an active displacer [2], and thus this served as an input for the passive displacer spring design. In order for the highest efficiency operation of the SPTC to be achieved, the correct phase angle between the displacer and the compressor is required. The right phase angle is given by the spring stiffness and the moving mass, and it should be approximately 45° for this displacer design, as demonstrated in Figure 2.

A plot of the von Mises stress acting on all regions of the spring is shown in Figure 5. The regions of highest stress in the spring are observed at:

- The 'teardrop' regions on the outskirts of the spring arm.
- The central part of the spring arms.

The spring stiffness was found to be approximately 1000 N/m. This was verified experimentally.

Spring Stiffness and Moving Mass

The springs utilized in the passive displacer require stiffness and fatigue testing in order to characterize their dynamics. The spring stiffness will allow for a decision to be made on the quantity of springs required in order to generate a given force. Measuring this experimentally allows for the simulated value through FE

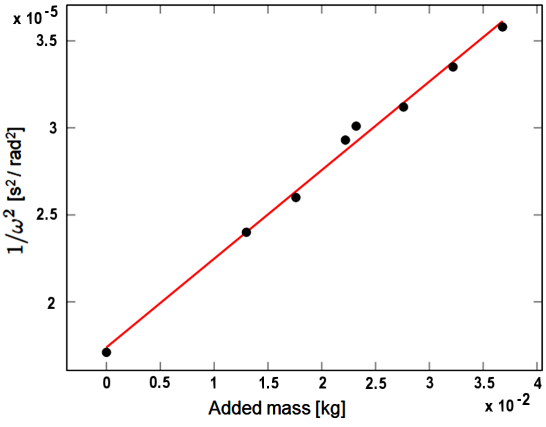

Figure 6. The reciprocal of the square of spring natural frequency against added mass to the spring.

analysis to be validated. This was done by incrementally adding masses to the spring and observing how the natural frequency of the spring, ω_n, at which the spring oscillates changes with each mass.

$$\omega_n^2 = k/m \quad (4)$$

Given Equation 4, plotting the reciprocal of frequency squared against the added mass, as shown in Figure 6, results in a gradient equating to $1/k$ and a y-intercept of k/m_0. Hence, the spring stiffness and the required moving mass of the displacer, m_0, can be determined. The values of k and m_0 were found to be approximately 1000 N/m and 34 g respectively.

Spring Fatigue Testing

The springs utilized in the passive displacer require stiffness and fatigue testing in order to better understand their mechanical characteristics. This allows for a decision to be made on the quantity of springs required to produce the right stiffness for the displacer motion. Figure 7 shows the setup of fatigue testing of the springs.

Two pairs of springs (4 in total) are mounted a small distance apart and connected directly to a moving magnet linear motor. The motor consists of an axially magnetized magnet placed in the middle of a pair of coils, each with 600 turns. An alternating current through the coils results in the oscillatory motion of the

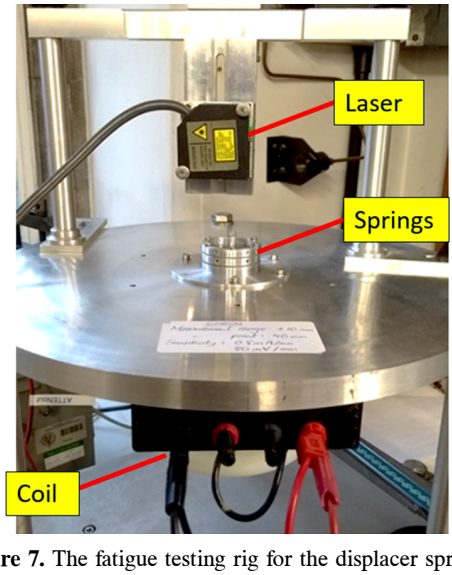

Figure 7. The fatigue testing rig for the displacer springs.

Table 1. Cycles completed at varying strokes by each batch of displacer springs and their failing strokes, for springs by manufacturers *A* and *B*.

Test batch	Cycles at 8 mm	Cycles at 10 mm	Cycles at 11 mm	Cycles at 12 mm	Failing stroke
A batch 1	10^7	10^7	10^7	2×10^5	12 mm
A batch 2	10^7	10^7	3×10^6	/	11 mm
B batch 1	10^7	5×10^6	/	/	10 mm
B batch 2	10^7	10^7	10^7	*ongoing*	≥12 mm

magnet linear motor to achieve an oscillatory stroke mimicking the motion of the springs in the displacer during operation. The springs are run at the maximum design stroke until 10^7 cycles have been completed. The stroke is then incrementally increased until failure occurs, allowing the safety margin of the spring design to be ascertained. An Omron displacement sensor is used to measure the oscillating spring displacement. The springs are run at approximately the resonant frequency, which increases slightly with each increase in stroke [4]. The frequency was within the range of 40-50 Hz.

Nominally identical spring sets from two different manufacturers, referred to in this paper as A and B, were tested. They each were 0.3 mm thick and had a design stroke of 8 mm. The key difference between the springs is the etching process used to manufacture them. Table 1 shows the results of the fatigue testing of both sets of springs, where upon the completion of 10^7 cycles the spring is considered to be able to run for infinite cycles (not failed). The results in Table 1 indicate that there appears to be variation in spring fatigue limit between batches and the manufacturer. All springs were operational beyond the displacer design stroke of 8 mm, and it is worth noting that the experimental displacer stroke operation is expected to run at a lower stroke of around 6 mm; hence showing a suitable margin for the displacer in question.

CONCLUSIONS AND NEXT STEPS

A passively run displacer for a coaxial SPTC has been designed. The spring stiffness, shaft diameter, and the moving mass required have been analytically determined through a range of analysis methods. The analytically obtained design parameters have been further verified experimentally. Further investigation into the surface properties of the springs to be used will be completed to better understand the discrepancies between the two spring manufacturers. This will shed light on the factors that most affect how the springs operate and respond to oscillatory loading. The experimental setup is due to be tested and the displacer design parameters may require iterative adjustments in order to achieve the highest SPTC efficiency.

ACKNOWLEDGMENTS

The authors would like to acknowledge partial funding from the EPSRC with EP/N017013/1 and Honeywell Hymatic for this project and broader SPTC research within the Cryogenic Engineering group at the University of Oxford. Furthermore, they would like to thank the reviewers of *Cryocoolers*.

REFERENCES

1. Zhu, S., "Pulse tube Stirling machines with warm gas-driven displacer," *Cryogenics*, vol. 50, no. 5 (2010), pp. 320-330.
2. Abolghasemi, M.A. et al., "Coaxial Stirling pulse tube cryocooler with active displacer," *Cryogenics*, vol. 111, (2020).
3. Radebaugh, R., "Thermodynamics of regenerative refrigerators," *Generation of Low Temperature and its Applications*, (2003).
4. Bailey, P.B. et al., "Low cost flexure spring testing," *IOP Conference Series: Materials Science and Engineering*, vol. 502 (2019).